BMC Medicine

RESEARCH ARTICLE

Open Access

Sustained correction of hippocampal neurogenic and cognitive deficits after a brief treatment by Nutlin-3 in a mouse model of fragile X syndrome

Sahar Javadi[1,2], Yue Li[1,3], Jie Sheng[1], Lucy Zhao[1], Yao Fu[1], Daifeng Wang[1,4] and Xinyu Zhao[1,5*]

Abstract

Background: Fragile X syndrome (FXS), the most prevalent inherited intellectual disability and one of the most common monogenic forms of autism, is caused by a loss of fragile X messenger ribonucleoprotein 1 (FMR1). We have previously shown that FMR1 represses the levels and activities of ubiquitin ligase MDM2 in young adult FMR1-deficient mice, and treatment by a MDM2 inhibitor Nutlin-3 rescues both hippocampal neurogenic and cognitive deficits in FMR1-deficient mice when analyzed shortly after the administration. However, it is unknown whether Nutlin-3 treatment can have long-lasting therapeutic effects.

Methods: We treated 2-month-old young adult FMR1-deficient mice with Nutlin-3 for 10 days and then assessed the persistent effect of Nutlin-3 on both cognitive functions and adult neurogenesis when mice were 6-month-old mature adults. To investigate the mechanisms underlying the persistent effects of Nutlin-3, we analyzed the proliferation and differentiation of neural stem/progenitor cells isolated from these mice and assessed the transcriptome of the hippocampal tissues of treated mice.

Results: We found that transient treatment with Nutlin-3 of 2-month-old young adult FMR1-deficient mice prevents the emergence of neurogenic and cognitive deficits in mature adult FXS mice at 6 months of age. We further found that the long-lasting restoration of neurogenesis and cognitive function might not be mediated by changing intrinsic properties of adult neural stem cells. Transcriptomic analysis of the hippocampal tissue demonstrated that transient Nultin-3 treatment leads to significant expression changes in genes related to the extracellular matrix, secreted factors, and cell membrane proteins in the FMR1-deficient hippocampus.

Conclusions: Our data indicates that transient Nutlin-3 treatment in young adults leads to long-lasting neurogenic and behavioral changes likely through modulating adult neurogenic niche that impact adult neural stem cells. Our results demonstrate that cognitive impairments in FXS may be prevented by an early intervention through Nutlin-3 treatment.

Keywords: Fragile X syndrome, FMR1, Nutlin-3, MDM2, Adult neurogenesis, Neural stem cells

Background

Fragile X Syndrome (FXS) is the most common cause of inherited intellectual disability with prevalence rates estimated to be 1:5000 in males and 1:8000 in females [1]. FXS is one of the most common single-gene causes of

*Correspondence: Xinyu.zhao@wisc.edu
[1] Waisman Center, University of Wisconsin-Madison, Madison, WI 53705, USA
Full list of author information is available at the end of the article

autism spectrum disorder (ASD), with approximately half of male FXS patients being clinically diagnosed with ASD [2, 3]. FXS is mainly caused by an expansion of trinucleotide repeats (CGG) to over 200 repeats in the 5′ untranslated region of the fragile X messenger ribonucleoprotein 1 (*FMR1*) gene which leads to transcriptional silencing of the gene with a subsequent reduction or absence of FMR1 (also known as FMRP, fragile X mental retardation protein) [4, 5]. FMR1 is a polyribosome-associated, brain-enriched, RNA-binding protein (RBP) that selectively targets specific mRNAs and regulates their translation, transport, stability, and nonsense-mediated RNA decay [4–9]. In addition, it has been shown that FMR1 is involved in histone modification and chromatin remodeling [10]. Hence, FMR1 is a multifunctional protein that could be involved in diverse biological processes.

FMR1 deficiency has been associated with numerous co-occurring conditions including, but not limited to, intellectual and emotional disabilities ranging from learning problems to mental retardation, and mood instability to autism [11]. A better understanding of the neurobiology and pathophysiology of FXS, together with advances in FXS animal models, has paved a way for the development of numerous targeted treatments for FXS [12]. FMR1 is a multifunctional protein that regulates the expression of a large number of direct and indirect targets [8, 13, 14]. Despite the rich literature aiming to investigate short-term therapeutic outcomes of treatments, very few studies have evaluated the potential long-lasting rescue effects of these treatments [12, 15]. Promising data from a recent study show that impairment of cognitive repertoire in FXS could be sustainably prevented by short-term pharmacological interventions [12, 16]. The long-lasting restoration of cognitive deficits of a rat model of FXS used in this study [12] is associated with sustained rescue of both synaptic plasticity and altered protein synthesis. These results have raised the question whether other reported interventions have the potential to exert long-lasting therapeutic effects.

Even though FMR1 is highly expressed in neurons, other cells have been implicated in FXS as well [17, 18]. Studies from our and other laboratories have shown that FMR1 regulates adult hippocampal neurogenesis [19–26]. Neurogenesis continuously occurs in at least two specific regions of the adult mammalian brain: the subventricular zone (SVZ) of the lateral ventricles and the subgranular zone (SGZ) of the dentate gyrus (DG) in the hippocampus [27]. Adult hippocampal neurogenesis is a multi-stage process, encompassing a number of developmental phases [27]. Activated neural stem cells (NSCs) or radial glia-like cells (RGLs) generate intermediate neural progenitors (NPs) that subsequently differentiate into neuroblasts, immature neurons, and mature granule neurons (GCs) that finally integrate into existing circuits [28]. Adult hippocampal neurogenesis is implicated in many functional processes such as learning, memory, plasticity, and mood regulation [27] and is impaired in a number of neurological conditions including FXS [19–26]. Therefore, interventions aimed at regulating adult neurogenesis are being evaluated as potential therapeutic strategies [29]. We have previously shown that the absence of FMR1 leads to increased NSC proliferation but reduced neuronal differentiation in young adult (2-month-old) *Fmr1* knockout (*Fmr1* KO) mice but reduced NSC proliferation and reduced neuronal differentiation in mature adult (6-month-old) *Fmr1* KO mice [20, 21]. At molecular levels, FMR1-deficient NSCs have elevated mouse double minute 2 (MDM2) protein levels and activities throughout adult ages. Treatment with Nutlin-3, a compound used for cancer clinical trial, specifically inhibits the interaction between MDM2 and its target proteins tumor protein P53 (TP53) and histone deacetylase 1 (HDAC1) and rescues both adult hippocampal neurogenic and behavioral deficits in both young adult and mature adult FXS mice. However, it remains unknown whether Nutlin-3 can have long-lasting effects in FXS mice, which is a key question for therapeutic development.

In this study, we investigated whether Nutlin-3 treatment had a sustained impact on neurogenesis and cognitive behaviors of FXS mice. We discovered that a transient treatment of young adult mice with Nutlin-3 led to a long-lasting effect in both hippocampal neurogenesis and cognitive tasks in adult FXS mice. To our surprise, we found that the long-lasting effect of Nutlin-3 might be mediated by regulating the gene expression of the adult stem cell niche rather than modulating the intrinsic properties of adult NSCs.

Methods

Study design

The purpose of this study was to investigate the long-lasting effect of Nutlin-3 treatment on impaired neurogenesis and behavioral deficits in adult FXS mice. In addition, we aimed to determine the potential mechanisms underlying the sustained rescue effect by Nutlin-3. Based on our publications and power analysis, at least three biological replicates were used for each in vitro or in vivo biochemical and histological analysis, whereas a sample size of 9 to 21 per group was used for behavioral testing. The NSPCs used for in vitro analyses were isolated from three pairs of *Fmr1* KO and WT littermates born to different parents, and NSPCs isolated from each animal were considered as a biological replicate. For drug treatment, animals were randomly assigned to treatment arms with approximately equivalent numbers in each group.

All cell counting and behavioral analyses were performed by experimenters who were blind to the identity of the samples.

Animal studies

All animal procedures were performed according to the protocols approved by the University of Wisconsin-Madison Institutional Animal Care and Use Committee. All mice were of C57B/L6 genetic background. The crossing and genotyping of these mice were carried out as described previously [20, 21]. Briefly, the *Fmr1* KO;*Nestin-GFP* mice (*Fmr1*$^{-/y}$;*Nestin-GFP*) were created by crossing female *Fmr1* heterozygous KO mice (*Fmr1*$^{+/-}$) [30] with homozygous *Nestin-GFP* transgenic males [31]. The generation of FMR1 inducible conditional mutant mice (*Fmr1*$^{loxP/y}$;*Nestin-CreER*^{T2};*Rosa26-tdT* or *cKO;Cre;Ai14*) and tamoxifen injections to induce recombination were performed as described [22]. To induce recombination, mice (6-7 week old) received tamoxifen (160 mg/kg; Sigma-Aldrich) daily for 5 days as described [22]. Nutlin-3 (10 mg/kg) was dissolved in dimethyl sulfoxide, given to 2-month-old mice through intraperitoneal injections every other day for five injections, and sacrificed at 4 months after the last injection. For in vivo differentiation analysis, mice also received four BrdU injections (100 mg/kg) within 12 h at 1 month before sacrifice.

Tissue preparation and immunohistochemistry

Brain tissue processing and histological analysis of mouse brains were performed as described in our publications [19–22, 32]. Briefly, mice were euthanized by intraperitoneal injection of a mixture of ketamine/xylazine/acepromazine followed by transcardiac perfusion with saline and then 4% paraformaldehyde (PFA). The brains were dissected out, post-fixed overnight in 4% PFA, and equilibrated in 30% sucrose. The brain sections of 40 μm thickness were generated using a sliding microtome and stored in a −20 °C freezer as floating sections in cryoprotectant solution (glycerol, ethylene glycol, and 0.1 M phosphate buffer (pH 7.4), 1:1:2 by volume). We performed immunohistological analysis on 1-in-6 serial floating brain sections (240 μm apart). After staining with primary and fluorescent secondary antibodies, the sections were counterstained with DAPI (1:1000; Roche Applied Science) and then mounted, coverslipped, and maintained at 4 °C in the dark until analysis.

The primary antibodies used were chicken anti-GFP (1:1000, Invitrogen, A10262), rabbit anti-MCM2 (1:500, Cell Signaling, 4007), rabbit anti-GFAP (1:1000, Dako, Z0334), mouse anti-GFAP (1:1000, Millipore, MAB360), mouse anti-NeuN (1:500, Millipore, MAB377), and rat anti-BrdU (1:1000, Abcam, ab6326).

Fluorescent secondary antibodies used were goat anti-mouse 568 (1:1000, Invitrogen, A11004), goat anti-rat 568 (1:1000, Invitrogen, A11077), goat anti-rabbit 568 (1:1000, Invitrogen, A11011), goat anti-rabbit 647 (1:1000, Invitrogen, A21245), goat anti-mouse 647 (1:1000, Invitrogen, A21235), goat anti-chicken 488 (1:1000, Invitrogen, A11039), and goat anti-mouse 488 (1:1000, Invitrogen, A11029).

In vivo cell quantification

Quantitative analyses of adult neurogenesis were carried out using an unbiased stereology method through the use of a Stereo Investigator software (MBF Biosciences) as described [20, 21, 33]. Briefly, Z-stack images (2-μm interval) were acquired using an AxioImager Z2 ApoTome confocal microscope (Plan-APOCHOROMAT, 20X, numerical aperture = 0.8; Zeiss). The measured thickness of the sections was ~ 30 μm. The cell numbers were quantified by random sampling one in six coronal serial sections (240 μm apart) encompassing the entire hippocampus, with 3-μm guard zones on each side. Schaeffer's coefficient of error (CE) < 0.1 was required for each type of cell quantification. The experimenter was blinded to the identity of the samples. The total numbers of GFP+GFAP+ cells in the dentate gyrus of each animal were counted. Then, the percentage of activated and proliferating NSCs was determined by co-localizing of GFP+GFAP cells with the cell cycle marker, MCM2. Cell lineage analysis was performed as described [20]. Briefly, at least 100 BrdU^{+} cells in the Z-stacks of each mouse were randomly selected, and their co-localization with cell-lineage marker, NeuN, was determined using Stereo Investigator.

Novel location recognition test

This test measures spatial memory through an evaluation of the ability of mice to recognize the new location of a familiar object with respect to spatial cues. The experimental procedure was carried out as described previously [20, 21]. Briefly, mice were handled for approximately 5 min a day for a maximum of 5 days prior to the experiment. Testing consisted of five 6-min trials, with a 3-min intertrial interval between each trial. All procedures were conducted during the light cycle of the animal between 10 a.m. and 4 p.m. Before the trial session, mice were brought into the testing room and were allowed to acclimate for at least 30 min. During the intertrial interval, the mouse was placed in a holding cage, which remained inside the testing room. In the first trial (pre-exposure), each mouse was placed individually in the center of the otherwise empty open arena (38.5 cm long × 38.5 cm wide, and 25.5-cm-high walls) for 6 min. For the next three trials (sample trials 13), two identical objects were

placed equidistantly from the arena wall in the corners against the wall with the colored decal. Tape the objects to the floor of the arena. Then, each mouse was placed individually in the center of the arena and was allowed to explore for 6 min. At the end of the trial, the mouse was removed and returned to the home cages for 3 min. In the last trial (test), one of the objects was moved to a novel location, and the mouse was allowed to explore the objects for 6 min, and the total time spent exploring each object was measured. During the test phase, the exploration time was defined as any investigative behavior (i.e., head orientation, climbing on, sniffing occurring within < 1.0 cm) or other motivated direct contact occurring with each object. To control for possible odor cues, objects were cleaned with 70% ethanol solution at the end of each trial, and the floor of the arena was wiped down to eliminate possible scent/trail markers. During the test phase, two objects were wiped down prior to testing so that the objects would all have the same odor. Based on a previous study [34], the discrimination index was calculated as the percentage of the time spent investigating the object in the new location minus the percentage of time spent investigating the object in the old location: discrimination index = (novel location exploration time/total exploration time × 100) − (old location exploration time/total exploration time × 100). A higher discrimination index is considered to reflect greater memory retention for the novel location object. All experiments were videotaped and scored by scientists who were blinded to the experimental conditions to ensure accuracy.

Novel object recognition test

This test is based on the natural propensity of rodents to preferentially explore the novel objects over familiar ones. The experimental procedure was carried out as described previously [20, 21]. Briefly, mice were handled for approximately 5 min a day for a maximum of 5 days prior to the experiment. The test was conducted during the light cycle of the animal between 10 a.m. and 4 p.m. Before the trial or test phase, mice were brought into the testing room and were allowed to acclimate for at least 30 min. On the first day, mice were habituated for 10 min to the V-maze, made out of black Plexiglas with two corridors (30 cm long × 4.5 cm wide, and 15-cm-high walls) set at a 90° angle, in which the task was performed. On the second day, mice were put back in the maze for 10 min, and two identical objects were presented. Twenty-four hours later, one of the familiar objects was replaced with a novel object, and the mice were again placed in the maze and were allowed to explore for 10 min, and the total time spent exploring each of the two objects (novel and familiar) was measured. During the test phase, the novel and familiar objects were wiped down prior to testing so that the objects would all have the same odor, and the exploration time was defined as the orientation of the nose to the object at a distance of less than 2 cm. The discrimination index was calculated as the difference between the percentages of the time spent investigating the novel object and the time spent investigating the familiar objects: discrimination index = (novel object exploration time/total exploration time × 100) − (familiar object exploration time/total exploration time × 100). A higher discrimination index is considered to reflect greater memory retention for the novel object. All experiments were videotaped and scored by scientists who were blinded to experimental conditions to ensure accuracy.

Adult NSPC isolation and analyses

NSPCs were isolated from the pooled DG tissue dissected from two 6-month-old male mice using our published method [21, 35]. NSPCs were cultured as described previously [35]. The proliferation and differentiation of NPCs were analyzed as described [20]. We used only early passage cells (between passages 4 and 10) and only the same passage numbers of wild-type and *Fmr1* KO cells for data collection. For each experiment, triplicate wells of cells (experimental replicates) were analyzed, and the results were averaged as one data point ($n = 1$). At least three independent biological replicates (cells isolated from different animals) were used ($n = 3$) for statistical analyses.

The primary antibodies used were mouse anti-Tuj1 (1:1000, Covance, 435P) and rat anti-BrdU (1:3000, Abcam, ab6326).

Fluorescent secondary antibodies used were goat anti-mouse 568 (1:2000, Invitrogen, A11004) and goat anti-rat 568 (1:2000, Invitrogen, A11077).

RNA isolation and RNA-seq

Freshly dissected hippocampal tissue was immediately frozen on dry ice. For RNA isolation, TRIzol was added to frozen tissue followed by homogenization using a Polytron (PT1200, Kinematica, Inc., Bohemia, NY, USA) as described [36]. RNA was isolated from TRIzol samples using the TRIzol Reagent following the manufacturer's instructions. RNA quality assessment, library construction, library quality control, and sequencing were performed by Novogene Bioinformatics Institute (Sacramento, CA, USA). Briefly, the quality, size, and concentration of the isolated RNA were analyzed using agarose gel electrophoresis, nanodrop, and an Agilent 2100 Bioanalyzer. Twelve cDNA libraries were constructed with three biological replicates for each condition: WT-Veh, KO-Veh, WT-Nut3, and KO-Nut3. Messenger RNA was purified from total RNA using poly-T oligo-attached magnetic beads. After fragmentation, the first-strand

cDNA was synthesized using random hexamer primers followed by the second strand cDNA synthesis. The library was ready after end repair, A-tailing, adapter ligation, size selection, amplification, and purification (Novogene, Sacramento, CA, USA). Library quality was assessed by Qubit 2.0, Agilent 2100, and qPCR. The libraries were clustered and sequenced on an Illumina Novaseq 6000 on an S4 flow cell. The 150-bp paired-end reads were generated after clustering of the index-coded samples. About 20–30 million reads were obtained for each sample.

Bioinformatics analysis

FastQC was used to perform a quality check of .fastq reads. Paired-end reads were mapped to the reference genome (mm10) using STAR (Additional file 1: STAR parameters). The raw count matrix was normalized by correcting for library size using the DESeq2 R package (Additional file 2: Code 2). The differential expression analysis was performed by using the DEseq2 R package (Additional file 2: Code 2). Adjusted *P*-values < 0.05 were used as cutoffs for differential expression. GO term enrichment was analyzed using Enricher (https://maayanlab.cloud/Enrichr) [37] and plotted using GOplot [38]. Differential expression was visualized by volcano plots (Additional file 3: Code 3). Transcription factor enrichment analysis and network were performed using ChEA3 (https://maayanlab.cloud/chea3) [39], and the average integrated ranks across all libraries RNA-seq data have been deposited to Gene Expression Omnibus (*GEO: GSE198403*).

Real-time PCR assay

Real-time PCR was performed using standard methods as described [20]. The first-strand cDNA was generated by reverse transcription with Oligo (dT) primer (Roche). To quantify the mRNA levels using real-time PCR, aliquots of first-stranded cDNA were amplified with gene-specific primers and Power SYBR Green PCR Master Mix (Bio-Rad) using a Step-1 Real-Time PCR System (Applied Biosystems). The PCR reactions contained 1 μg of cDNA, Universal Master Mix (Applied Biosystems), and 10μM of forward and reverse primers in a final reaction volume of 20 μL. The data analysis software built-in with the 7300 Real-Time PCR System calculated the mRNA level of different samples. The sequences of primers used for real-time PCR reactions in mouse species are listed in Additional file 4: Table S1.

Western blotting analyses

Protein samples were separated on SDS-PAGE gels (Bio-Rad), transferred to the PVDF membranes (Millipore), and incubated with primary antibodies. The antibodies include p-MDM2 (Ser166,1:1000, Novus Biologicals, NBP1-51396), HDAC1 (1:1000, BioVersion, 3601-30), Acetyl-H3 (1:1000,Millipore, 06-599), Histone H3 (1:1000, Cell Signaling, 9715S), P53 (1:1000, Santa Cruz, sc-6243), EP300 (1:1000, Novus Biologicals, NB100-616), and GAPDH (1:5000,Thermo Scientific, MA5-15738). After incubation with fluorescence-labeled secondary antibodies (Li-CoR), the membranes were imaged using Li-CoR, and quantification was performed using the Image Studio Lite software. The amount of loading protein (20 μg) was determined by the linear range of the target proteins (10–40 μg) using the Li-CoR system as previously described [20]. At least three independent blots were used for statistical analysis.

Statistical analysis

All experiments were randomized and blinded to scientists who performed the quantification. Statistical analysis was performed using ANOVA and Student's *t*-test, unless specified, with the GraphPad Prism software 9. Two-tailed and unpaired *t*-test was used to compare two conditions. Two-way ANOVA with Tukey's post hoc analysis was used for analyzing multiple groups. All data were shown as mean with standard error of the mean (mean ± SEM). Probabilities of $P < 0.05$ were considered as significant.

Results

Transient Nutlin-3 treatment has a long-lasting rescue effect on impaired hippocampal neurogenesis in *Fmr1* KO mice

We have previously shown that young adult (2-month-old) *Fmr1* KO mice exhibited elevated NSC activation and impaired neurogenesis, and mature adult (6-month-old) *Fmr1* KO mice exhibited reduced NSC activation and impaired neurogenesis in the hippocampus, which can be normalized to WT levels immediately after a 10-day treatment by a specific MDM2 inhibitor Nutlin-3 [20, 21]. To assess the potential of MDM2 inhibition as a therapeutic treatment, a critical question remained whether the Nutlin-3 treatment has long-lasting rescue effects. We thus decided to investigate whether a transient Nutlin-3 treatment could have a persistent therapeutic effect on NSC activation and adult neurogenesis in FXS mouse models.

We crossed *Fmr1* mutant mice with *Nestin*-GFP (green fluorescent protein) mice in which GFP expression is driven by the promotor of a neural stem and progenitor cell marker NESTIN to create the *Fmr1* KO;*Nestin-GFP* double transgenic mice as described previously [20]. We treated 2-month-old *Fmr1* KO (*Fmr1*$^{-/y}$;*Nestin-GFP*) and littermate wild-type (*Fmr1*$^{+/y}$;*Nestin-GFP*) mice with either vehicle or Nutlin-3 (10 mg/kg) every other day over

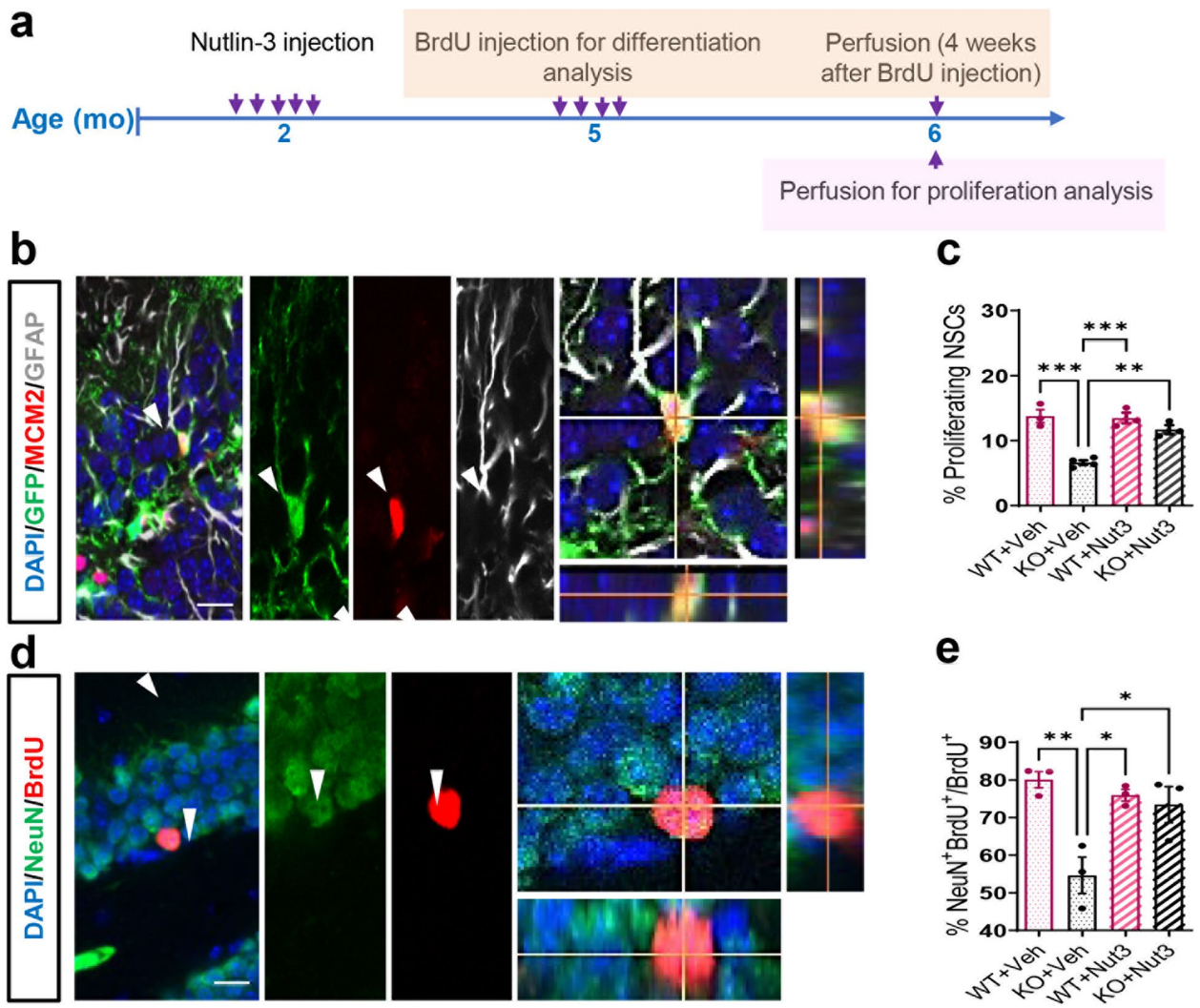

Fig. 1 Transient treatment with Nutlin-3 has a long-lasting rescue effect on impaired hippocampal neurogenesis in FMR1-deficient mice. **a** Experimental scheme for assessing the hippocampal neurogenesis in *Fmr1* KO and WT mice treated with Nutlin-3 (Nut3) or vehicle (Veh). **b** Sample confocal images used for identifying NSCs (GFP+GFAP+) and proliferating NSCs (GFP+GFAP+MCM2+) in the DG of adult *Fmr1* KO and WT mice bred into a *Nestin-GFP* mouse background. Scale bar, 20 μm. **c** Comparison of the percentage of activated NSCs among total NSCs in the DG of *Fmr1* KO and WT mice with or without Nutlin-3 treatment ($n = 3$ or 4 per group). **d** Sample confocal images to identify new mature neurons (NeuN+BrdU+) in the dentate gyrus of *Fmr1* KO and WT mice. Scale bar, 20 μm. **e** Comparison of the percentage of mature neurons among BrdU+ cells in DG of *Fmr1* KO and WT mice with or without Nutlin-3 treatment ($n = 3$ per group). $^{*}P < 0.05$; $^{**}P < 0.01$; $^{***}P < 0.001$. Data are presented as means ± SEM

10 days (total 5 injections) as we have done previously [20, 21] and analyzed them at 4 months after the last injections, when the mice were 6 months old (Fig. 1a). Glial fibrillary acidic protein (GFAP) is a radial glia marker expressed in both quiescent and activated adult hippocampal NSCs (Fig. 1b) [40]. To determine the activation of NSCs, we used the cell cycle marker minichromosome maintenance complex component 2 (MCM2; Fig. 1b). We quantified the percentage of activated ($GFP^{+}GFAP^{+}MCM2^{+}$) NSCs over total ($GFP^{+}GFAP^{+}$) NSCs in *Fmr1* KO and WT mice. We found that *Fmr1* KO mice treated with vehicle at 2 months of age exhibited reduced NSC activation at 6 months of age compared to WT with the same vehicle treatment (Fig. 1c), which is consistent with our previous finding on 6-month-old *Fmr1* KO mice [21]. Similarly to what we have published before [20, 21], Nutlin-3 treatment had no significant effect on WT mice (Fig. 1c). In contrast, *Fmr1* KO mice treated with Nutlin-3 at 2 months of age showed no significant difference in NSC activation at 6 months of age

compared to WT mice treated with either vehicle or Nutlin-3 (Fig. 1c). Therefore, a 10-day transient Nutlin-3 treatment of young adult *Fmr1* KO mice has a long-lasting rescue effect on adult hippocampal NSC activation, which persists for at least 4 months.

We then assessed whether the therapeutic effect of Nutlin-3 on neuronal differentiation [20, 21] could persist long after treatment. Thus, we injected 2-month-old *Fmr1* KO ($Fmr1^{-/y}$) mice and WT ($Fmr1^{+/y}$) littermates with Nutlin-3 as described above (Fig. 1a) [20]. At 5 months of age, the mice received four injections of a synthetic thymidine analog bromodeoxyuridine (BrdU) over a 12-h period to pulse label proliferating NSCs and progenitors in the adult DG and were sacrificed at 4 weeks after BrdU injections (6 months of age) for differentiation analysis (Fig. 1a) [20]. To identify the fate of the BrdU-labeled NSPCs, we performed co-immunostaining using antibodies against mature neuronal marker NeuN (neuronal nuclei antigen or RBFOX3) and BrdU and quantified the percentage of neuronal differentiation ($BrdU^+NeuN^+/BrdU^+$) (Fig. 1d). We found that *Fmr1* KO mice treated with vehicle showed a significant reduction in neuronal differentiation compared to WT counterparts treated with either vehicle or Nutlin-3 (Fig. 1e), which is consistent with what has been reported previously [21]. In contrast, 6-month-old *Fmr1* KO mice treated with Nutlin-3 at 2 months of age showed elevated neuronal differentiation levels comparable to that of the WT mice (Fig. 1e). Nutlin-3 administration did not show significant effects on neurogenesis of WT mice (Fig. 1e). Therefore, transient treatment of *Fmr1* KO mice with Nutlin-3 at young adult ages could prevent impairment of neuronal differentiation in mature adult mice. In summary, our findings have revealed a long-lasting therapeutic effect of Nutlin-3 on impaired NSC activation and neuronal differentiation in a FXS mouse model.

Transient Nutlin-3 treatment has an endured corrective effect on cognitive deficit in FXS mouse models

We have previously shown that *Fmr1* KO mice exhibited deficits in hippocampus-dependent cognitive functions [20–22, 41] and Nutlin-3 treatment reversed impaired spatial learning assessed by a novel location recognition test (NLR) and defective cognitive function assessed by a novel object recognition (NOR) test at 1 month after treatment [20, 21]. Since our current study has revealed a persistent therapeutic effect of Nutlin-3 on impaired NSC activation and neurogenesis in *Fmr1* KO mice (Fig. 1), we decided to investigate whether the Nutlin-3-dependent restoration of cognitive deficit is also long-lasting.

First, to confirm that selective deletion of FMR1 from NSCs in young adult mice leads to long-lasting impaired performances on hippocampus-dependent learning tasks, we generated tamoxifen-inducible *Fmr1* conditional knockout ($cKO;CreER^{T2}$;Ai14) triple transgenic mice by crossing *Fmr1*-floxed ($Fmr1^{f/f}$ or cKO) mice with inducible *Nestin* promotor-driven Cre transgenic mice ($Nes\text{-}CreER^{T2}$) and *Rosa26-STOP-tdTomato* (Ai14) reporter mice as described previously [20] (Additional file 9: Fig. S1a). We found that targeted deletion of FMR1 from NSCs and their progenies at 2 months of age led to learning deficits at 6 months of age (Additional file 9: Fig. S1b-d), which corroborated our previous findings [20, 22]. More importantly, transient treatment of $cKO;CreER^{T2};Ai14$ mice with Nutlin-3 at 2 months of age led to the restoration of cognitive function when assessed at 6 months of age (Additional file 9: Fig. S1b-d). Therefore, transient Nutlin-3 treatment in young adult mice with selective deletion of FMR1 from adult new neurons has a long-lasting effect.

We then treated 2-month-old *Fmr1* KO mice and their WT littermates with either vehicle or Nutlin-3 and analyzed their behaviors 4 months later (Fig. 2a). Consistent with our previous findings, *Fmr1* KO mice treated with vehicle exhibited impaired performance in spatial learning on the NLR test and defective learning on the NOR test (Fig. 2b–e) [21]. In contrast, Nutlin-3 administration rescued the impaired performances of *Fmr1* KO mice in both NLR (Fig. 2c) and NOR (Fig. 2e) to the wild-type levels without significant effect on wild-type mice (Fig. 2c, e). Therefore, a transient Nutlin-3 treatment of FMR1-deficient mice at young adulthood could rescue impaired cognitive performance for at least 4 months.

Transient treatment with Nutlin-3 does not have a persistent effect on intrinsic properties of adult neural stem/progenitor cells

We next sought to reveal the molecular mechanisms that are associated with Nutlin-3-induced enduring rescue of impaired hippocampal neurogenesis and related cognitive functions. Adult NSCs and adult hippocampal neurogenesis are regulated by both intrinsic and extrinsic factors [42]. To determine whether Nutlin-3 treatment acted through the NSC intrinsic pathways, we decided to analyze the neural stem/progenitor cells (NSPCs) isolated from the hippocampus of 6-month-old *Fmr1* KO and littermate WT mice treated with either vehicle or Nutlin-3 at 2 months of age (Fig. 3a) using our published methods [35]. We used BrdU pulse labeling to assess NSPC proliferation and found that *Fmr1* KO NSPCs exhibited a reduced BrdU incorporation rate compared to WT NSPCs (Fig. 3b, d), consistent with our published results on NSPCs isolated from 6-month-old *Fmr1 KO* mice [21]. Surprisingly, Nutlin-3 treatment did not rescue the impaired proliferation of *Fmr1* KO cells (Fig. 3d). We then assessed NPSC neuronal differentiation using

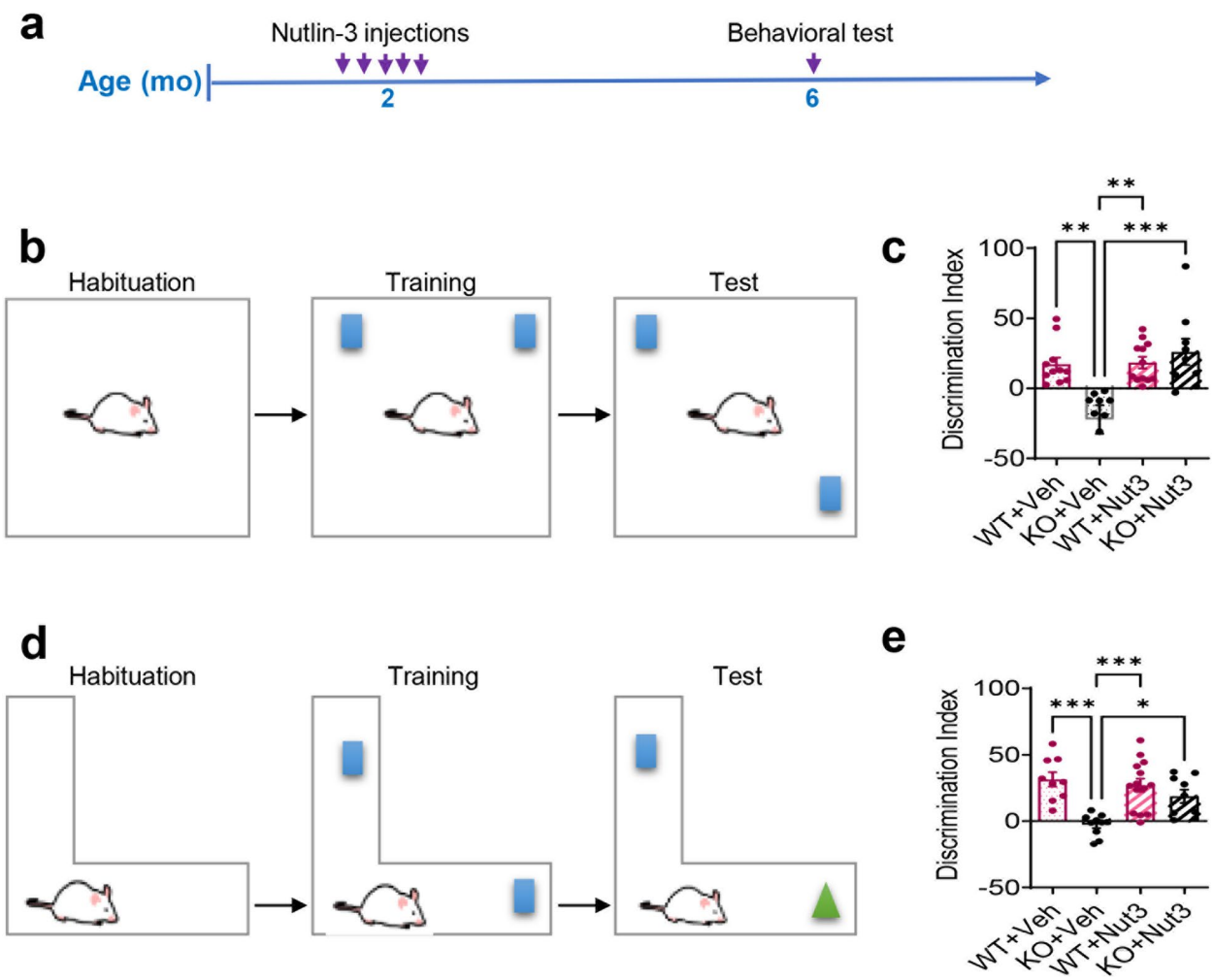

Fig. 2 Transient treatment with Nutlin-3 has a long-lasting rescue effect on cognitive deficits in FMR1-deficient mice. **a** Experimental scheme for analyzing cognitive performances in *Fmr1* KO and WT mice treated with Nutlin-3 (Nut3) or vehicle (Veh). **b** Schematic of novel location recognition (NLR) test for assessing spatial learning. **c** Beneficial effects of Nutlin-3 treatment on spatial memory deficits in *Fmr1* KO mice sustained at least 4 months after injection ($n = 8$ to 13 mice per group). **d** Schematic of the novel object recognition (NOR) test. **e** Therapeutic effects of Nutlin-3 treatment on deficits in the NOR test in *Fmr1* KO mice last at least for 4 months after treatment cessation ($n = 8$ to 13 mice per group). *$P < 0.05$; **$P < 0.01$; ***$P < 0.001$. Data are presented as means ± SEM

(See figure on next page.)

Fig. 3 Transient treatment with Nutlin-3 does not have a persistent effect on intrinsic properties of adult neural stem/progenitor cells. **a** Experimental scheme for analyzing proliferation and differentiation of hippocampal NSPCs isolated from *Fmr1* KO and WT mice treated with Nutlin-3 (Nut3) or vehicle (Veh). **b** Sample images of proliferating NSPCs pulse-labeled with thymidine analog, BrdU followed by immunohistology for in vitro quantification assay. Red, BrdU; blue, DAPI; scale bar, 20 µm. **c** Sample images of differentiating NSPCs assessed by immunohistological detection of a neuronal marker $Tuj1^+$ for in vitro quantification of NSPC neuronal differentiation. Red, Tuj1; blue, DAPI; scale bar, 20 µm. **d**, **e** Nutlin-3 treatment did not rescue impaired proliferation (**d**) and neuronal differentiation (**e**) of hippocampal NSPCs isolated from *Fmr1* KO and WT mice 4 months after injection ($n = 3$). **f**, **g** Western blot analysis of P-MDM2 levels in isolated NSPCs isolated from *Fmr1* KO and WT 4 months after Nutlin-3 or vehicle treatment ($n = 3$). **h**–**k** Western blot analysis of the total histone H3 (T-H3), acetylated histone H3 (acetyl-H3), and HDAC1 levels in NSPCs isolated from *Fmr1* KO and WT mice 4 months after Nutlin-3 or vehicle treatment ($n = 3$). **l**, **m** Western blot analysis of P53 levels in isolated NSPCs isolated from *Fmr1* KO and WT 4 months after Nutlin-3 or vehicle treatment ($n = 3$). **n**, **o** Western blot analysis of EP300 levels in isolated NSPCs isolated from *Fmr1* KO and WT 4 months after Nutlin-3 or vehicle treatment ($n = 3$). Glyceraldehyde-3-phosphate dehydrogenase (GAPDH) was used as loading controls. Due to the large size of EP300, loading controls were run on a separate gel. *$P < 0.05$; **$P < 0.01$; ***$P < 0.001$. Data are presented as means ± SEM

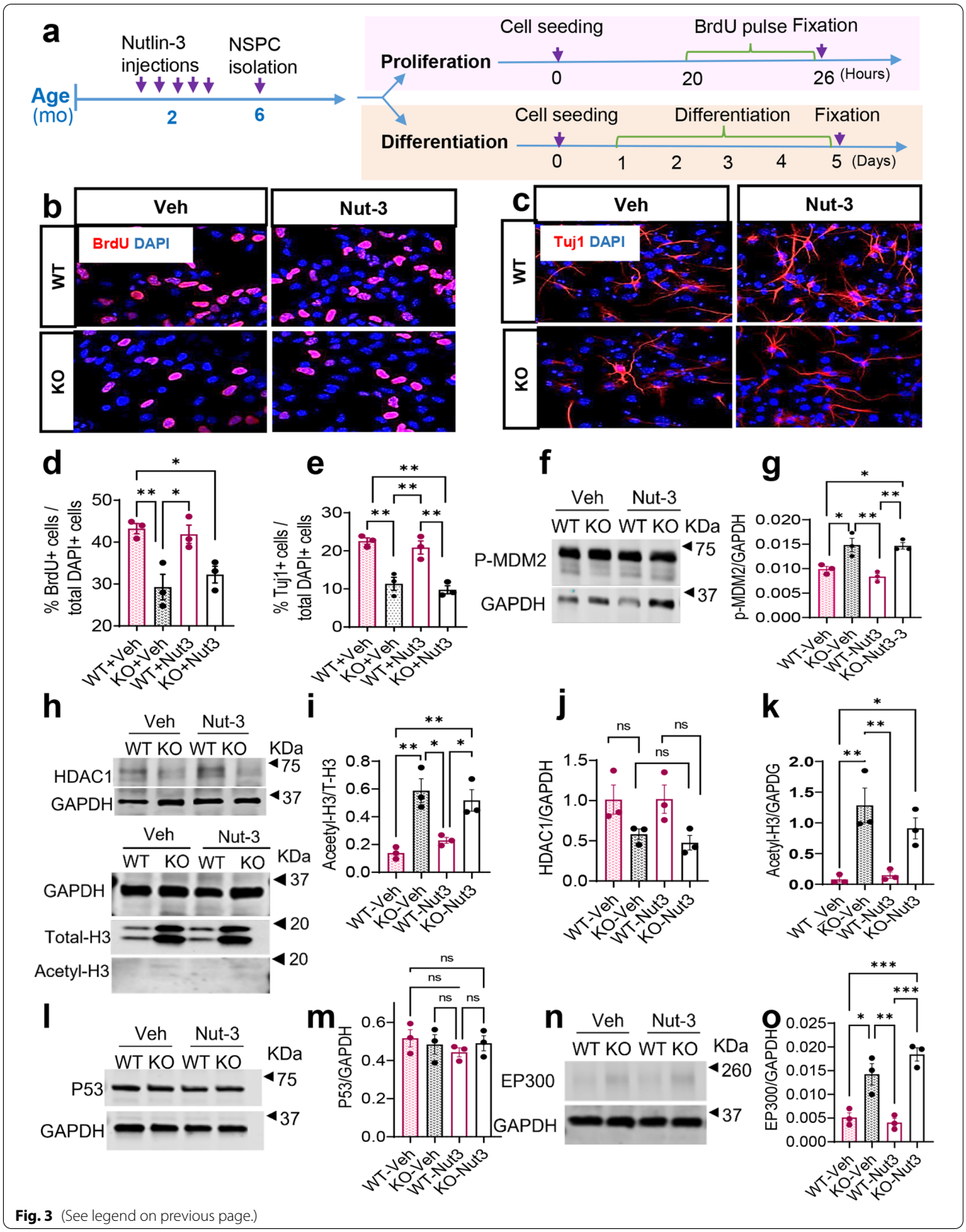

Fig. 3 (See legend on previous page.)

an antibody for immature neuron, βIII-tubulin (Tuj1), and found that NSPCs isolated from *Fmr1* KO mice at 4 months after either Nutlin-3 or vehicle injection exhibited similarly reduced neuronal differentiation (Fig. 3c, e). We have previously shown that NSCs isolated from 6-month-old mice exhibited elevated levels of phosphorylated MDM2 (P-MDM2, the active form of MDM2), EP300, acetylated Histone H3, and HDAC1, a target of MDM2 in 6-month-old mice [21], but not protein levels of P53, a target of MDM2 in NSCs in 2-month-old mice [20]. We therefore assessed the levels of these proteins and found that NSPCs isolated from KO mice exhibited increased P-MDM2 and EP300 protein levels, elevated H3 acetylation, and reduced HDAC1 levels, without significant change in P53 levels (Fig. 3f–o), consistent with our published results [21]. More importantly, treatment of Nutlin-3 at 2 months of age did not alter the levels of these proteins in the NSPCs isolated from 6-month-old mice (Fig. 3f–o). Therefore, these data suggest that the long-lasting effect of Nutlin-3 on hippocampal NSPCs might not lead to changes in the intrinsic properties of NSPCs.

Transient Nutlin-3 treatment leads to significant and specific gene expression changes in Fmr1 KO hippocampus

Since transient Nutlin-3 treatment did not have a significant rescue effect on NSPCs isolated 4 months later, we reckoned that Nutlin-3 might exert its long-lasting impact on hippocampal neurogenesis through modulating stem cell niche in the hippocampus. Indeed, Nutlin-3 treatment had a persistent effect on reducing H3 acetylation in hippocampal and cortex tissue of *Fmr1*-KO mice (Additional file 9: Fig. S2). To explore the potential regulatory mechanisms, we injected 2-month-old *Fmr1* KO and WT control mice with Nutlin-3 or vehicle and harvested the hippocampi at 4 months post-treatment for transcriptomic analysis in triplicates (Fig. 4a). Total sequencing reads generated for each sample were between 21 and 26 million ($21 \times 10^6 < TRs < 26 \times 10^6$) (Additional file 5: Table S2). More than 94% of reads were uniquely mapped to the mouse genome, which corresponds to more than 25×10^3 genes (Additional files 5 and 6: Tables S2 and S3). We evaluated the distribution of read counts across the samples and found that the overall density distribution of raw log intensities exhibited a highly consistent pattern (Additional file 9: Fig. S3).

Next, we performed differential expression analysis to identify differentially regulated genes (DEGs) among the four experimental groups. Adjusted *P*-values < 0.05 were used as cutoffs for the differential expression. We identified no DEG between vehicle-treated and Nutlin-3-treated WT (WT-Veh vs WT-Nut3) mice, consistent with a lack of effect by Nutlin-3 on WT mice shown in our published results [20, 21] and current neurogenic and behavioral data (Figs. 1, 2, 3, and 4b–d; Additional file 9: Fig. S4, Additional file 7: Table S4). We identified 21 DEGs between vehicle-treated *Fmr1* KO (KO-Veh) and WT mice (WT-Veh), of which 13 DEGs were downregulated and 8 genes were upregulated (Fig. 4d; Additional file 9: Fig. S4, Additional file 7: Table S4). Surprisingly, we found that the most significant gene expression changes were between vehicle-treated and Nulin-3-treated *Fmr1* KO mice (KO-Veh vs KO-Nut3) (Fig. 4c,d; Additional file 7: Table S4). Out of a total of 237 DEGs (KO-Veh vs KO-Nut3), 6 genes were downregulated and 231 genes were upregulated in Nutlin-3-treated KO mice (Fig. 4d,e; Additional file 7: Table S4). Only 1 DEG, gene Gm21887 or *Erdr1* (erythroid differentiation regulator 1), was shared between these two groups of DEGs and was downregulated in KO-Veh both groups (Fig. 4c; Additional file 7: Table S4). Therefore, transient Nutlin-3-triggered significant gene expression changes in KO mice but did not make gene expression in KO mice to be more comparable to that in WT mice.

To understand the biological significance of DEGs found in *Fmr1* KO mice treated with Nutlin-3, we performed Gene Ontology (GO) analysis using three categories of term analysis: biological pathway, cell component, and molecular function (Additional file 8: Table S5). We generated circle plots to demonstrate the specific enrichment and the directionality of the gene expression changes within each GO category (Fig. 5a). The DEGs were generally enriched for extracellular matrix, cell membrane proteins, and secreted factors (Fig. 5a; Additional file 8: Table S5) known to be the key components of the adult neurogenic niche [43–46], including the well-known bone morphogenetic protein (BMP) and

(See figure on next page.)

Fig. 4 Transient treatment with Nutlin-3 leads to long-lasting gene expression changes in the hippocampus of FMR1-deficient mice. **a** Experimental timeline for sample collection and transcriptomic profiling of the hippocampal tissue of *Fmr1* KO and WT mice injected with Nutlin-3 (Nut3) or vehicle (Veh) ($n = 3$ per group). **b** *M-A* plot of *M* (log ratio) and *A* (mean average) displaying $\log_2$ fold change of genes compared with the mean expression levels of all genes with $\log_2$ fold change thresholds between −3 and 3. The genes identified differential expression (adjusted $P < 0.05$) are indicated as blue dots. **c** Volcano plot showing the gene fold changes and adjusted *P*-values between KO-Veh and KO-Nutl3 groups. The most upregulated genes are towards the right, the most downregulated genes are towards the left, and the most statistically significant genes are towards the top. The red points are the genes with adjusted *P*-value < 0.05. **d** Venn diagram showing the overlap patterns of differentially expressed genes between the different experimental groups. **e** The numbers of up (blue) and down (red) regulated genes between KO-Veh and WT-Veh and between KO-Nut3 and KO-Veh

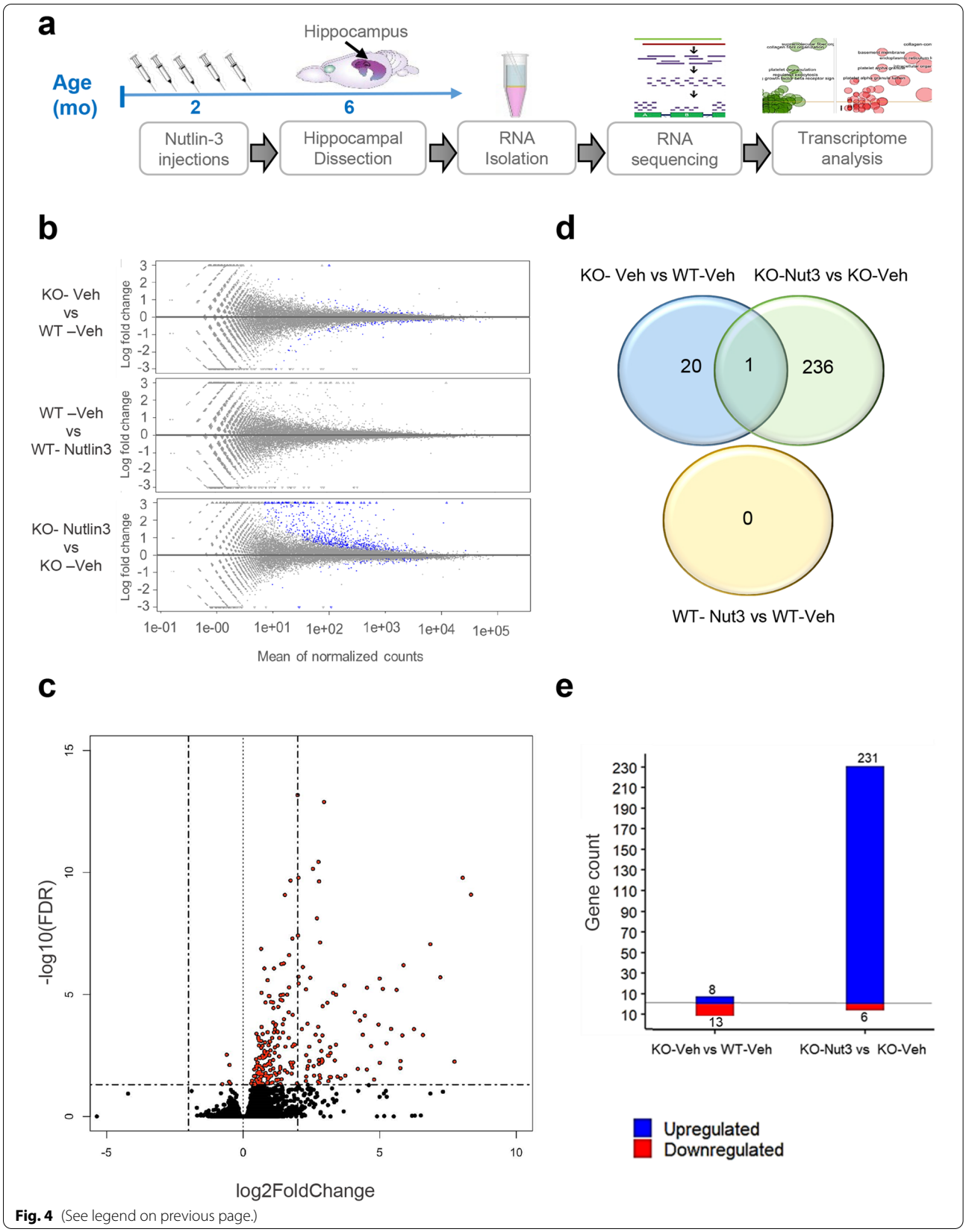

Fig. 4 (See legend on previous page.)

transforming growth factor beta (TGFß) signaling pathway [47] and insulin-like growth factor 2 (IGF2) pathway [48]. In each GO category, there was a robust upregulation of the DEGs for the enriched terms (Fig. 5a).

Because the enriched terms have shown strong potential in stem cell regulation through modulating stem cell niche [43–46], we next selected a number of candidate DEGs from each group and validated their differential expression in KO-Nut3 compared to KO-Veh using quantitative polymerase chain reaction (qPCR) analysis. Administration of Nutlin-3 in *Fmr1* KO mice led to significant changes in the expression levels of genes associated to extracellular matrix (*Col8a1* and *Timp3*), cell membrane (*Aqp1* and *Tmem72*), and secreted factors (*Angptl2*, *Enpp2*, *BMP6*, and *Igf2*) and the only DEG shared between the two groups (*Erdr1*), compared to WT littermates (Fig. 5b–k).

To further explore how these gene expression changes might have happened, we next performed transcription factor (TF) target enrichment analysis to identify potential upstream TFs responsible for observed changes in the gene expression of Nutlin-3-treated *Fmr1* KO mice. Our analysis showed that the top TFs are mainly involved in stem cell fate specification (such as MEOX1, MEOX2, PRRX1, BNC2, SOX18, and TWIST1) [49–53] and/or extracellular matrix organization (such as HEYL, TBX18, PRRX1, PRRX2, and TCF21) [54–56] (Fig. 6a; Additional file 9: Fig. S5). We then assessed the relationship among our top TFs using a published TF network. We found that our top TFs related to Nutlin-3 treatment in KO mice showed a high level of interactions (Fig. 6b). Together, our transcriptomic analysis of the hippocampal tissue supports that the long-lasting rescue effects of Nutlin-3 treatment on impaired adult neurogenesis and dependent cognitive functions of *Fmr1* KO mice might be through modulating the adult NSC niche.

Discussion

This study sought to test the hypothesis that transient therapeutic intervention can produce long-lasting beneficial effects on cognitive functions in a mouse model of FXS. Our results demonstrate that a transient Nutlin-3 treatment of young adults for 10 days restored impaired hippocampal neurogenesis and related cognitive abilities in *Fmr1* KO mouse for at least 4 months after treatment cessation. Together with our publications [20, 21], these findings indicate that not only brief Nutlin-3 treatment rescues the neurogenic and cognitive deficits in adult FXS mice, but also these beneficial effects are sustained long after the end of treatment. Our data also suggest that Nutlin-3 treatment during the early adulthood time window might establish the normal adult NSC niche required for intact neurogenesis and cognitive performances in the absence of FMR1.

Numerous therapeutic alternatives including newly developed compounds or repurposed drugs have been proposed for FXS [20, 57]. There are many advantages of drug repurposing in the treatment of disease, including shortening the time frame and reducing the cost associated with new drug development [58]. When assessing the feasibility of initiating treatments, an obvious concern is the resulting toxicity from long-term administration. For these reasons, there has been extensive interest in the possibility of repurposing drugs with potentially long-lasting therapeutic effects. However, only very few studies have assessed the persistent effect of treatment long after treatments are stopped. In a recent study, the minocycline treatment effect has lasted for 4 weeks in young FXS mice but not in adult FXS mice [15]. In another study, transient treatment of FXS rats with lovastatin at 4 weeks of age for 5 weeks prevented the emergence of cognitive deficits in object-place recognition and object-place-context recognition [12]. The authors show that the corrective effect has been sustained for at least 3 months (the last time point tested) after treatment termination, and the observed restoration of normal cognitive function is associated with sustained rescue of both synaptic plasticity and altered protein synthesis [12]. One promising candidate for drug repurposing is a group of MDM2 inhibitors, and its prototype is Nutlin-3. Nutlin-3 is a small molecule that specifically inhibits MDM2, an E3 ubiquitin ligase, and the best known MDM2 targets are tumor suppressor TP53; therefore, Nutlin-3 and its derivative have been worked on extensively and used in clinical trials for cancer treatment [59]. Our lab has found that, in adult NSPCs, FMR1 directly regulates the

(See figure on next page.)

Fig. 5 Differentially expressed genes in FMR1-deficient mice treated with Nutlin-3 were enriched for genes associated with regulation of adult neural stem cell niche. **a** Bubble plots for Gene Ontology (GO) analysis showing enriched terms identified with Enricher for DEGs between *Fmr1* KO treated with either Nutlin-3 or vehicle. The results of three different categories of GO analysis are shown. The size of the bubbles indicates the number of genes. The *x*-axis indicates the *z* score (negative = downregulated in Nutlin-3-treated *Fmr1* KO mice; positive = upregulated in Nutlin-3-treated *Fmr1* KO mice). The *y*-axis indicates the negative logarithm of adjusted *P*-value from GO analysis (higher = more significant). ECM organization, membrane proteins, and secreted factors are the top hits in each GO category. **b** Heat map of the transcriptional changes of selected DEGs between Nutlin-3 and vehicle-treated *Fmr1* KO mice, revealed by RNA-seq ($n = 3$) and quantitative PCR (qPCR) analysis ($n = 4$). Red and green represent upregulation and downregulation, respectively. **c**–**k** Quantitative PCR analysis to validate a subset of DEGs in each GO category including Angptl2 (**c**), Aqp1 (**d**), Bmp6 (**e**), Col8a1 (**f**), Enpp2 (**g**), Erdr1 (**h**), Igf2 (**i**), Tmp3 (**j**), and Tmem72 (**k**) ($n = 3$/condition). The mRNA levels of glyceraldehyde-3-phosphate dehydrogenase (GAPDH) were used as the internal control. *$P < 0.05$; **$P < 0.01$; ***$P < 0.001$. Data are presented as means ± SEM

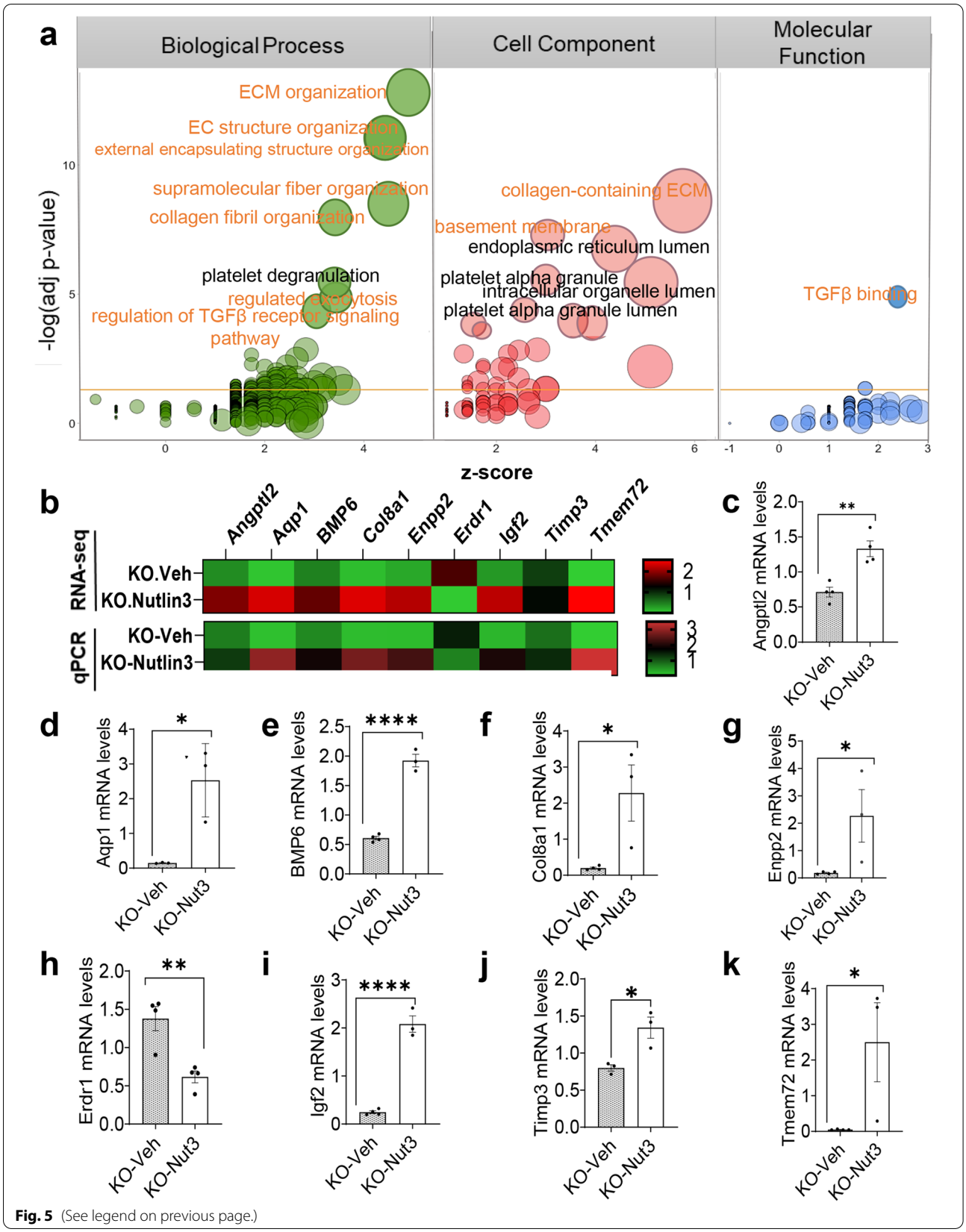

Fig. 5 (See legend on previous page.)

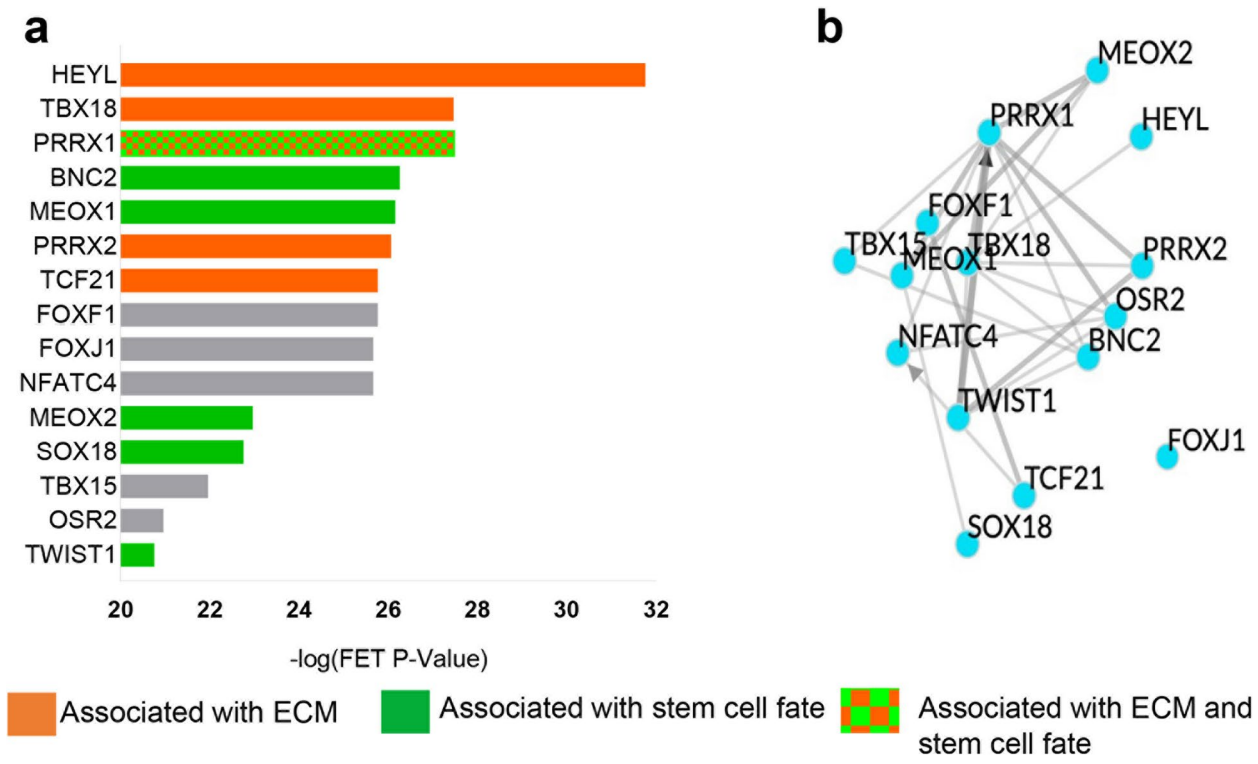

Fig. 6 Top TFs ranked by TF enrichment analysis were associated to ECM and stem cell fate. **a** Transcription factor target enrichment analysis of differentially expressed genes in *Fmr1* KO treated with Nutlin-3 vs vehicle using average integrated ranks across all libraries through ChEA3 ($n = 3$). FET, Fisher's exact test. Orange bars indicate TFs associated with ECM. Green bars indicate TFs associated with stem cell fate. Orange and green patterned bars indicate TFs associated to both ECM and stem cell function, respectively. **b** top TF network generated by Chea3 using the average integrated ranks across all libraries

expression levels and activities of MDM2, which targets TP53 and HDAC1 [20, 21]. Our published studies have shown that Nutlin-3 administration at a dosage significantly lower than those used for cancer treatment rescues impaired hippocampal neurogenesis and cognitive functions in both 2-month-old young adult FXS mice and 6-month-old mature adult FXS mice analyzed shortly after the treatment [20, 21]. However, the long-lasting effect of Nutlin-3 was unknown. Our current study has addressed this important question and taken one step further to potential therapeutic applications of MDM2 inhibition for the treatment of FXS.

Understanding the molecular mechanism underlying drug action is important for both therapeutic application and improvement of drug development. To investigate the mechanism underlying the long-lasting effect of Nutlin-3, we first determined whether this effect was due to the persistent changes in intrinsic properties of NSCs by using primary NSPCs isolated from *Fmr1* KO or WT mouse hippocampus. We have previously shown that NSPCs isolated from 2-month-old *Fmr1* KO hippocampus had reduced *TP53* gene expression, increased proliferation, and reduced neuronal differentiation, which can be corrected by Nutlin-3 treatment [20]. *TP53* gene encodes a transcription factor TP53 regulating a network of target genes that play roles in various cellular processes including but limited to apoptosis, cell cycle arrest, genomic integrity, metabolism, redox biology, and stemness [60]. Tp53 binds DNA in a sequence-specific manner and recruits transcriptional machinery components to activate or suppress the expression of a network of target genes [61]. TP53 has also been shown to regulate gene expression through epigenetic mechanisms [62–64], which may lead to long-lasting alteration in the gene expression. We therefore hypothesized that Nutlin-3 treatment may exert a sustained therapeutic effect on the FXS mouse model through modulating epigenetic pathways in NSPCs. To our surprise, our results indicate that transient Nutlin-3 treatment did not lead to persistent corrections in active MDM2 levels nor proliferation and differentiation of NSPCs isolated from 6-month-old *Fmr1* KO mice. This suggests that, unlike the immediate response to Nutlin-3 treatment, the long-lasting therapeutic effect of Nutlin-3 on neurogenesis might not act mainly through modulating NSPC intrinsic properties [20, 21]. Because

adult neurogenesis is regulated by both NSC intrinsic pathways and extrinsic stem cell niche [65], we performed gene expression profile analysis of *Fmr1* KO and WT hippocampal tissue. Nutlin-3 treatment exerted minimal change in the gene expression profile of WT hippocampus which is supported by our previous findings [20, 21]. On the other hand, Nultlin-3-treated KO mice mounted persistent and significant gene expression changes compared to vehicle-treated KO mice and WT mice. However, Nutlin-3 treatment did not make KO more similar to WT in the gene expression profile. This observation suggests that the low-dosage Nutlin-3 we used was effective in rebalancing cellular pathways in the absence of FMR1 but had no significant effect on WT because the cellular pathways were well regulated by the presence of FMR1. Among DEGs, we found mRNAs of proteins associated to the extracellular matrix, cell membrane, and secreted factors, many of which have been shown to regulate adult neurogenesis [44–46]. For example, genes in TGFß and BMP signaling are upregulated in Nutlin-3-treated KO mice, which we have confirmed using qPCR. It has been shown that TGFß and BMP activation in adult NSC niche can activate adult neurogenesis [66, 67]. In addition, *Igf2* mRNA expression levels were significantly higher in the Nutlin-3-treated KO hippocampus compared to either vehicle-treated KO hippocampus or WT mice. IGF2 has also been shown to promote adult NSC proliferation and neurogenesis [48]. It is possible that the Nutlin-3 has an effect on both niche cells and NSCs, but the long-lasting effects of Nutlin-3 on NSCs can only be observed in the presence of niche cells, which explains why we saw rescue in mice with NSC-targeted FMR1 deletion. Furthermore, since Nutlin-3 was given systemically, we do not rule out that the Nutlin-3 effect might in part act through modulating peripheral systems.

One potential limitation of this study is that we have not defined whether an age range or a critical period exists for the initial Nutlin-3 treatment to achieve the long-lasting effectiveness of Nutlin-3 treatment. Future experiments on Nutlin-3 administration time at younger or older ages than 2 months should be considered. In addition, we showed that the beneficial effects of Nutlin-3 on impaired neurogenesis and cognition of FXS mice sustained for at least 4 months. Whether the effect lasts for a longer period or even for the rest of the animal's life will need to be addressed in future studies. Furthermore, we have assessed adult neurogenesis-dependent behaviors. It is possible that Nutlin-3 also improves other aspects of behavioral deficits in FXS mice which is independent of adult neurogenesis; therefore, it will be beneficial to assess whether the beneficial effects of Nutlin-3 can be generalized to other forms of cognitive and behavior functions found in FXS. Although our transcriptomic analysis has provided an important clue for the long-term effect of Nutlin-3 treatment, a comprehensive assessment of the gene expression and epigenetic profiles of neurogenic niche will be needed to fully understand the molecular basis of the persistent effect of Nutlin-3. Finally, humans and rodents have distinct physiology, lifespan, and genetics [68]. Whether Nutlin-3 treatment can have therapeutic effects on human FXS remains unknown. Although we observed that the effect of Nutlin-3 lasted 4 months which is a long time for mice with a lifespan of 2 years, human has a much longer lifespan and different metabolic rate. Translating our results into human treatment will need substantial further investigations.

Conclusions

In summary, our findings indicate that a brief Nutlin-3 treatment of young adult FXS mice has a long-lasting therapeutic effect on both neurogenesis and behaviors and that the sustained beneficial effect might be exerted through modulating the adult NSC niche. Our observation strengthens the idea that Nutlin-3 is one of the ideal candidates for optimal therapy with minimal toxicity in a targeted therapeutic approach. The findings provide proof-of-concept evidence that FXS, and perhaps neurodevelopmental disorders more generally, may be amenable to transient, early intervention to permanently restore normal cognitive functions.

Abbreviations

ASD: Autism spectrum disorder; ANOVA: Analysis of variance; BrdU: Bromodeoxyuridine; cKO: Conditional knockout; DEG: Differentially expressed gene; CE: Coefficient of error; DG: Dentate gyrus; ECM: Extracellular matrix; Erdr1: Erythroid differentiation regulator 1; Fig: Figure; *Fmr1*: Fragile X mental retardation protein 1; FMR1: Fragile X messenger ribonucleoprotein 1; FMRP: Fragile X mental retardation protein (previous name); FXS: Fragile X syndrome; GAPDH: Glyceraldehyde-3-phosphate dehydrogenase; GC: Granule cell; GFP: Green fluorescent protein; GFAP: Glial fibrillary acidic protein; GO: Gene ontology; HDAC1: Histone deacetylase 1; KO: Knockout; qPCR: Quantitative polymerase chain reaction; MCM2: Minichromosome maintenance complex component 2; MDM2: Mouse double minute 2; NeuN: Neuronal nuclei antigen; NIH: National Institute of Health; NLR: Novel location recognition; NOR: Novel object recognition; NSPC: Neural stem/progenitor cell; NSC: Neural stem cell; NP: Neural progenitors; Nut3: Nutlin3; p53: Protein; PFA: Paraformaldehyde; RBFOX3: RNA-binding fox-1 homolog 3; RGL: Radial glial like; SGZ: Subgranular zone; SVZ: Subventricular zone; TF: Transcription factor; Veh: Vehicle; WT: Wild-type.

Supplementary Information

The online version contains supplementary material available at https://doi.org/10.1186/s12916-022-02370-9.

Additional file 1: Code S1. Parameters for STAR alignment.

Additional file 2: Code S2. R codes for differentially expressed gene analysis.

Additional file 3: Code S3. R Codes for volcano plot.

Additional file 4: Table S1. Primer sequences for qPCR.

Additional file 5: Table S2. Result of RNA-seq read alignment.

Additional file 6: Table S3. Raw read counts of RNA-seq samples.

Additional file 7: Table S4. Differentially expressed genes among experimental groups.

Additional file 8: Table S5. GO enrichment analysis results

Additional file 9: Fig. S1. Transient treatment with Nutlin-3 has long-lasting rescue effect on cognitive deficits in mice with selective deletion of Fmr1 in adult new neurons. **Fig. S2.** Acetylated Histone H3 levels in the hippocampus and the cortex. **Fig. S3.** Boxplot to show the density distribution of raw log-intensities of RNA-seq data of all samples. **Fig. S4.** Volcano plots showing gene fold changes and adjusted P-values between different conditions. **Fig. S5.** GO analysis of top upstream TF.

Acknowledgements
We thank Y. Xing, K.A. Schoeller, J. Le, G.J. Lawrence, and S. Sharma for the technical assistance; J. Panksepp, D. Bolling, MM Eastwood, and K. Knobel at the Waisman IDD Model Core for the services; and UW-Madison Biotechnology Center for the next-generation sequencing services.

Authors' contributions
XZ conceived the concept. XZ, SJ, and YL designed and performed the experiments, collected the data, and analyzed the data. LZ and YF collected the data. SJ and XZ wrote the manuscript. JS and DW performed the bioinformatics analysis. All authors read and approved the final manuscript.

Funding
This work was supported by grants from the National Institutes of Health (R01MH118827, R01MH116582, and R01NS105200 to X.Z.; R01NS064025, R01AG067025, and U01MH116492 to D.W.; U54HD090256 and P50HD105353 to the Waisman Center), Jenni and Kyle Professorship to XZ, and Wisconsin Distinguished Graduate Fellowship to SJ.

Availability of data and materials
All data and materials are available by contacting Dr. Xinyu Zhao (xinyu.zhao@wisc.edu). The next-generation sequencing data is available through Gene Expression Omnibus (*GEO: GSE198403*).

Declarations

Ethics approval and consent to participate
All animal experiments have been approved by the Institutional Animal Care and Use Committee at the University of Wisconsin-Madison.

Consent for publication
The authors agree to publish this work.

Competing interests
XZ and YL are inventors of a patent ("Methods for treating cognitive deficits associated with fragile x syndrome" United States US 9,962,380 B2). The remaining authors declare that they have no competing interests.

Author details
[1]Waisman Center, University of Wisconsin-Madison, Madison, WI 53705, USA. [2]Department of Animal Sciences, College of Agriculture and Life Sciences, University of Wisconsin-Madison, Madison, WI 53705, USA. [3]Present address: Institute of Traditional Chinese Medicine, Tianjin University of Traditional Chinese Medicine, Tianjin 301617, China. [4]Department of Biostatistics and Medical Informatics, School of Medicine and Public Health, University of Wisconsin-Madison, Madison, WI 53705, USA. [5]Department of Neuroscience, School of Medicine and Public Health, University of Wisconsin-Madison, Madison, WI 53705, USA.

Received: 5 January 2022 Accepted: 6 April 2022
Published online: 13 May 2022

References

1. Tassone F, Iong KP, Tong T-H, Lo J, Gane LW, Berry-Kravis E, et al. FMR1 CGG allele size and prevalence ascertained through newborn screening in the United States. Genome Med. 2013;4(12):1–13.
2. Budimirovic DB, Kaufmann WE. What can we learn about autism from studying fragile X syndrome? Dev Neurosci. 2011;33(5):379–94.
3. Kaufmann WE, Kidd SA, Andrews HF, Budimirovic DB, Esler A, Haas-Givler B, et al. Autism spectrum disorder in fragile X syndrome: cooccurring conditions and current treatment. Pediatrics. 2017;139(Supplement 3):S194–206.
4. Pieretti M, Zhang F, Fu Y-H, Warren ST, Oostra BA, Caskey CT, et al. Absence of expression of the FMR-1 gene in fragile X syndrome. Cell. 1991;66(4):817–22.
5. Verkerk AJ, Pieretti M, Sutcliffe JS, Fu Y-H, Kuhl DP, Pizzuti A, et al. Identification of a gene (FMR-1) containing a CGG repeat coincident with a breakpoint cluster region exhibiting length variation in fragile X syndrome. Cell. 1991;65(5):905–14.
6. De Rubeis S, Bagni C. Fragile X mental retardation protein control of neuronal mRNA metabolism: insights into mRNA stability. Mol Cell Neurosci. 2010;43(1):43–50.
7. Bassell GJ, Warren ST. Fragile X syndrome: loss of local mRNA regulation alters synaptic development and function. Neuron. 2008;60(2):201–14.
8. Richter JD, Zhao X. The molecular biology of FMRP: new insights into fragile X syndrome. Nat Rev Neurosci. 2021;22(4):209–22.
9. Kurosaki T, Imamachi N, Proschel C, Mitsutomi S, Nagao R, Akimitsu N, et al. Loss of the fragile X syndrome protein FMRP results in misregulation of nonsense-mediated mRNA decay. Nat Cell Biol. 2021;23(1):40–8.
10. Alpatov R, Lesch BJ, Nakamoto-Kinoshita M, Blanco A, Chen S, Stützer A, et al. A chromatin-dependent role of the fragile X mental retardation protein FMRP in the DNA damage response. Cell. 2014;157(4):869–81.
11. Garber KB, Visootsak J, Warren ST. Fragile X syndrome. Eur J Hum Genet. 2008;16(6):666–72.
12. Asiminas A, Jackson AD, Louros SR, Till SM, Spano T, Dando O, et al. Sustained correction of associative learning deficits after brief, early treatment in a rat model of Fragile X Syndrome. Sci Transl Med. 2019;11(494). https://doi.org/10.1126/scitranslmed.aao0498.
13. Richter JD, Bassell GJ, Klann E. Dysregulation and restoration of translational homeostasis in fragile X syndrome. Nat Rev Neurosci. 2015;16(10):595–605.
14. Ascano M, Mukherjee N, Bandaru P, Miller JB, Nusbaum JD, Corcoran DL, et al. FMRP targets distinct mRNA sequence elements to regulate protein expression. Nature. 2012;492(7429):382–6.
15. Dansie LE, Phommahaxay K, Okusanya AG, Uwadia J, Huang M, Rotschafer SE, et al. Long-lasting effects of minocycline on behavior in young but not adult Fragile X mice. Neuroscience. 2013;246:186–98.
16. Ligsay A, Hagerman RJ. Review of targeted treatments in fragile X syndrome. Intractable Rare Dis Res. 2016;5(3):158–67. https://doi.org/10.5582/irdr.2016.01045.
17. Bakker CE, de Diego OY, Bontekoe C, Raghoe P, Luteijn T, Hoogeveen AT, et al. Immunocytochemical and biochemical characterization of FMRP, FXR1P, and FXR2P in the mouse. Exp Cell Res. 2000;258(1):162–70.
18. Devys D, Lutz Y, Rouyer N, Bellocq J-P, Mandel J-L. The FMR–1 protein is cytoplasmic, most abundant in neurons and appears normal in carriers of a fragile X premutation. Nat Genet. 1993;4(4):335–40.
19. Luo Y, Shan G, Guo W, Smrt RD, Johnson EB, Li X, et al. Fragile x mental retardation protein regulates proliferation and differentiation of adult neural stem/progenitor cells. PLoS Genet. 2010;6(4).
20. Li Y, Stockton ME, Bhuiyan I, Eisinger BE, Gao Y, Miller JL, et al. MDM2 inhibition rescues neurogenic and cognitive deficits in a mouse model of fragile X syndrome. Sci Transl Med. 2016;8(336):336ra61.
21. Li Y, Stockton ME, Eisinger BE, Zhao Y, Miller JL, Bhuiyan I, et al. Reducing histone acetylation rescues cognitive deficits in a mouse model of Fragile X syndrome. Nat Commun. 2018;9(1):1–16.
22. Guo W, Allan AM, Zong R, Zhang L, Johnson EB, Schaller EG, et al. Ablation of Fmrp in adult neural stem cells disrupts hippocampus-dependent learning. Nat Med. 2011;17(5):559–65.
23. Liu B, Li Y, Stackpole EE, Novak A, Gao Y, Zhao Y, et al. Regulatory discrimination of mRNAs by FMRP controls mouse adult neural stem cell differentiation. Proc Natl Acad Sci. 2018;115(48):E11397–E405.
24. Pinar C, Yau S-y, Sharp Z, Shamei A, Fontaine CJ, Meconi AL, et al. Effects of voluntary exercise on cell proliferation and neurogenesis in the dentate gyrus of adult FMR1 knockout mice. Brain Plast. 2018;4(2):185–95.

25. Lazarov O, Demars MP, Da Tommy ZK, Ali HM, Grauzas V, Kney A, et al. Impaired survival of neural progenitor cells in dentate gyrus of adult mice lacking fMRP. Hippocampus. 2012;22(6):1220–4.
26. Eadie B, Zhang W, Boehme F, Gil-Mohapel J, Kainer L, Simpson J, et al. Fmr1 knockout mice show reduced anxiety and alterations in neurogenesis that are specific to the ventral dentate gyrus. Neurobiol Dis. 2009;36(2):361–73.
27. Kempermann G, Song H, Gage FH. Neurogenesis in the adult hippocampus. Cold Spring Harbor Perspect Biol. 2015;7(9):a018812.
28. Eisch AJ, Cameron HA, Encinas JM, Meltzer LA, Ming G-L, Overstreet-Wadiche LS. Adult neurogenesis, mental health, and mental illness: hope or hype? J Neurosci. 2008;28(46):11785–91.
29. Babcock KR, Page JS, Fallon JR, Webb AE. Adult hippocampal neurogenesis in aging and Alzheimer's disease. Stem Cell Rep. 2021;16(4):681–93.
30. Consortium TD-BFX. Fmr1 knockout mice: a model to study fragile X mental retardation. The Dutch-Belgian Fragile X Consortium. Cell. 1994;78(1):23–33.
31. Yamaguchi M, Saito H, Suzuki M, Mori K. Visualization of neurogenesis in the central nervous system using nestin promoter-GFP transgenic mice. Neuroreport. 2000;11(9):1991–6.
32. Guo W, Zhang L, Christopher DM, Teng Z-Q, Fausett SR, Liu C, et al. RNA-binding protein FXR2 regulates adult hippocampal neurogenesis by reducing Noggin expression. Neuron. 2011;70(5):924–38.
33. Zhao X, van Praag H. Steps towards standardized quantification of adult neurogenesis. Nat Commun. 2020;11(1):4275.
34. Contestabile A, Greco B, Ghezzi D, Tucci V, Benfenati F, Gasparini L. Lithium rescues synaptic plasticity and memory in Down syndrome mice. J Clin Investig. 2012;123(1).
35. Guo W, Patzlaff NE, Jobe EM, Zhao X. Isolation of multipotent neural stem or progenitor cells from both the dentate gyrus and subventricular zone of a single adult mouse. Nat Protoc. 2012;7(11):2005.
36. Gao Y, Shen M, Gonzalez JC, Dong Q, Kannan S, Hoang JT, et al. RGS6 mediates effects of voluntary running on adult hippocampalneurogenesis. Cell Rep. 2020;32(5):107997.
37. Chen EY, Tan CM, Kou Y, Duan Q, Wang Z, Meirelles GV, et al. Enrichr: interactive and collaborative HTML5 gene list enrichment analysis tool. BMC Bioinformatics. 2013;14:128.
38. Walter W, Sanchez-Cabo F, Ricote M. GOplot: an R package for visually combining expression data with functional analysis. Bioinformatics. 2015;31(17):2912–4.
39. Keenan AB, Torre D, Lachmann A, Leong AK, Wojciechowicz ML, Utti V, et al. ChEA3: transcription factor enrichment analysis by orthogonal omics integration. Nucleic Acids Res. 2019;47(W1):W212–W24.
40. Kempermann G, Jessberger S, Steiner B, Kronenberg G. Milestones of neuronal development in the adult hippocampus. Trends Neurosci. 2004;27(8):447–52.
41. Guo W, Murthy AC, Zhang L, Johnson EB, Schaller EG, Allan AM, et al. Inhibition of GSK3β improves hippocampus-dependent learning and rescues neurogenesis in a mouse model of fragile X syndrome. Hum Mol Genet. 2012;21(3):681–91.
42. Eisinger BE, Zhao X. Identifying molecular mediators of environmentally enhanced neurogenesis. Cell Tissue Res. 2018;371(1):7–21.
43. Scadden DT. The stem-cell niche as an entity of action. Nature. 2006;441(7097):1075–9.
44. Moore KA, Lemischka IR. Stem cells and their niches. Science. 2006;311(5769):1880–5.
45. Lutolf MP, Blau HM. Artificial stem cell niches. Adv Mater. 2009;21(32-33):3255–68.
46. Kjell J, Fischer-Sternjak J, Thompson AJ, Friess C, Sticco MJ, Salinas F, et al. Defining the adult neural stem cell niche proteome identifies key regulators of adult neurogenesis. Cell Stem Cell. 2020;26(2):277–93. e8.
47. Zhang J, Li L. BMP signaling and stem cell regulation. Dev Biol. 2005;284(1):1–11.
48. Ziegler AN, Feng Q, Chidambaram S, Testai JM, Kumari E, Rothbard DE, et al. Insulin-like growth factor II: an essential adult stem cell niche constituent in brain and intestine. Stem Cell Rep. 2019;12(4):816–30.
49. Sutcu HH, Ricchetti M. Loss of heterogeneity, quiescence, and differentiation in muscle stem cells. Stem Cell Invest. 2018;5.
50. Stevanovic M, Drakulic D, Lazic A, Ninkovic DS, Schwirtlich M, Mojsin M. SOX transcription factors as important regulators of neuronal and glial differentiation during nervous system development and adult neurogenesis. Front Mol Neurosci. 2021;14:51.
51. Francois M, Caprini A, Hosking B, Orsenigo F, Wilhelm D, Browne C, et al. Sox18 induces development of the lymphatic vasculature in mice. Nature. 2008;456(7222):643–7.
52. Shimozaki K, Clemenson GD, Gage FH. Paired related homeobox protein 1 is a regulator of stemness in adult neural stem/progenitor cells. J Neurosci. 2013;33(9):4066–75.
53. Panman L, Andersson E, Alekseenko Z, Hedlund E, Kee N, Mong J, et al. Transcription factor-induced lineage selection of stem-cell-derived neural progenitor cells. Cell Stem Cell. 2011;8(6):663–75.
54. Silva AC, Pereira C, Fonseca ACR, Pinto-do-Ó P, Nascimento DS. Bearing my heart: the role of extracellular matrix on cardiac development, homeostasis, and injury response. Front Cell Dev Biol. 2021;8:1705.
55. Hall BK, Miyake T. All for one and one for all: condensations and the initiation of skeletal development. Bioessays. 2000;22(2):138–47.
56. Hu H, Lin S, Wang S, Chen X. The role of transcription factor 21 in epicardial cell differentiation and the development of coronary heart disease. Front Cell Dev Biol. 2020;8:457.
57. Berry-Kravis EM, Lindemann L, Jønch AE, Apostol G, Bear MF, Carpenter RL, et al. Drug development for neurodevelopmental disorders: lessons learned from fragile X syndrome. Nat Rev Drug Discov. 2018;17(4):280–99.
58. Tranfaglia MR, Thibodeaux C, Mason DJ, Brown D, Roberts I, Smith R, et al. Repurposing available drugs for neurodevelopmental disorders: the fragile X experience. Neuropharmacology. 2019;147:74–86.
59. Secchiero P, Bosco R, Celeghini C, Zauli G. Recent advances in the therapeutic perspectives of Nutlin-3. Curr Pharm Des. 2011;17(6):569–77.
60. Rufini A, Tucci P, Celardo I, Melino G. Senescence and aging: the critical roles of p53. Oncogene. 2013;32(43):5129–43.
61. Beckerman R, Prives C. Transcriptional regulation by p53. Cold Spring Harbor Perspect Biol. 2010;2(8):a000935.
62. Sheikh T, Sen E. p53 affects epigenetic signature on SOCS1 promoter in response to TLR4 inhibition. Cytokine. 2021;140:155418.
63. Tovy A, Spiro A, McCarthy R, Shipony Z, Aylon Y, Allton K, et al. p53 is essential for DNA methylation homeostasis in naïve embryonic stem cells, and its loss promotes clonal heterogeneity. Genes Dev. 2017;31(10):959–72.
64. Levine AJ, Berger SL. The interplay between epigenetic changes and the p53 protein in stem cells. Genes Dev. 2017;31(12):1195–201.
65. Kempermann G. Seven principles in the regulation of adult neurogenesis. Eur J Neurosci. 2011;33(6):1018–24.
66. Kandasamy M, Lehner B, Kraus S, Sander PR, Marschallinger J, Rivera FJ, et al. TGF-beta signalling in the adult neurogenic niche promotes stem cell quiescence as well as generation of new neurons. J Cell Mol Med. 2014;18(7):1444–59.
67. Bond AM, Peng CY, Meyers EA, McGuire T, Ewaleifoh O, Kessler JA. BMP signaling regulates the tempo of adult hippocampal progenitor maturation at multiple stages of the lineage. Stem Cells. 2014;32(8):2201–14.
68. Zhao X, Bhattacharyya A. Human models are needed for studying human neurodevelopmental disorders. Am J Hum Genet. 2018;103(6):829–57.

Publisher's Note